Ultrafine-Grained AlCoCrFeNi2.1 Eutectic High-Entropy Alloy

Materials Research Letters

ISSN: (Print) 2166-3831 (Online) Journal homepage: https://www.tandfonline.com/loi/tmrl20

Ultrafine-Grained $AlCoCrFeNi_{2.1}$ Eutectic High-Entropy Alloy

I. S. Wani, T. Bhattacharjee, S. Sheikh, Y. P. Lu, S. Chatterjee, P. P. Bhattacharjee, S. Guo & N. Tsuji

To cite this article: I. S. Wani, T. Bhattacharjee, S. Sheikh, Y. P. Lu, S. Chatterjee, P. P. Bhattacharjee, S. Guo & N. Tsuji (2016) Ultrafine-Grained $AlCoCrFeNi_{2.1}$ Eutectic High-Entropy Alloy, Materials Research Letters, 4:3, 174-179, DOI: 10.1080/21663831.2016.1160451

To link to this article: https://doi.org/10.1080/21663831.2016.1160451

Published online: 25 Mar 2016.

MATERIALS RESEARCH LETTERS

Mater. Res. Lett., 2016
Vol. 4, No. 3, 174–179, http://dx.doi.org/10.1080/21663831.2016.1160451

Taylor & Francis
Taylor & Francis Group

www.tandfonline.com/toc/tmrl20/current

Ultrafine-Grained AlCoCrFeNi$_{2.1}$ Eutectic High-Entropy Alloy

I. S. Wani[a], T. Bhattacharjee[b], S. Sheikh[c], Y. P. Lu[d], S. Chatterjee[a], P. P. Bhattacharjee[a]*, S. Guo[c] and N. Tsuji[b,e]

[a]*Department of Materials Science and Metallurgical Engineering, IIT Hyderabad, Kandi 502 285, Telangana, India;* [b]*Department of Materials Science and Engineering, Kyoto University, Yoshida Honmachi, Sakyo-ku, Kyoto, 606-8501 Japan;* [c]*Department of Materials and Manufacturing Technology, Chalmers University of Technology, SE-41296 Gothenburg, Sweden;* [d]*Key Laboratory of Solidification Control and Digital Preparation Technology (Liaoning Province), School of Materials Science and Engineering, Dalian University of Technology, Dalian 116024, People's Republic of China;* [e]*Elements Strategy Initiative for Structural Materials (ESISM), Kyoto University, Japan*

(*Received 5 February 2016; final form 27 February 2016*)

The development of microstructure and mechanical properties was investigated in a heavily cold-rolled and annealed AlCoCrFeNi$_{2.1}$ high-entropy alloy. The as-cast alloy having a eutectic morphology consisting of alternate bands of ordered L1$_2$ and B2 phases was 90% cold-rolled. The deformed microstructure showed profuse shear banding and disordering of the L1$_2$, but no transformation of the B2 phase. A duplex microstructure consisting of ultrafine equiaxed grains ($\sim$0.60 µm) of disordered face centered cubic and B2 was observed after annealing at 800°C. The annealed material showed remarkable strength–ductility combination having ultimate tensile strength $\sim$1.2 GPa and elongation to failure $\sim$12%.

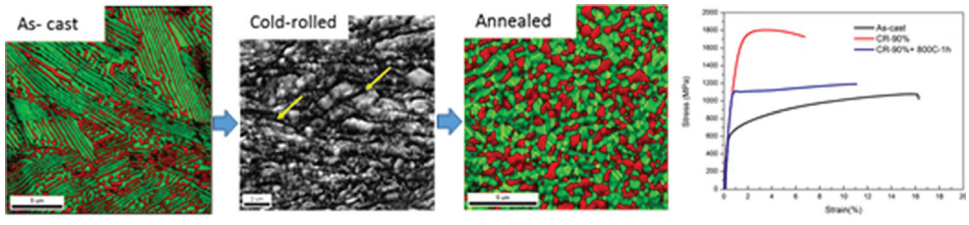

Keywords: High-Entropy Alloys, Ordered Phases, Cold-Rolling, Annealing, Properties

Impact Statement: AlCoCrFeNi$_{2.1}$ eutectic HEA with ordered L1$_2$ and B2 phases can be thermo-mechanically processed to achieve ultrafine structure and remarkable strength-ductility properties.

High-entropy alloys (HEAs) are multicomponent alloys originally based on the novel alloy design approach of mixing five or more elements in equiatomic or near-equiatomic proportions.[1] Despite the presence of several constituents, the HEAs can show the presence of single phases with simple structure such as FCC or BCC, or FCC + BCC.[1] This has been attributed to the high entropy of mixing of a large number of components in equiatomic or near-equiatomic proportions, which effectively reduces the free energy.[1,2] However, recent investigations have shown that high entropy of mixing alone is not sufficient to explain the phase formation in HEAs. For example, equiatomic HEAs with the same number of constituents may consist of multiple phases depending on the constituent elements,[3] while non-equiatomic alloys can exist as single-phase solid solution having simple structures,[4] Therefore, the phase formation in HEAs is guided not only by the number of components (i.e. configurational entropy), but also by the type of the constituent elements. The definition and rules governing the phase formation in HEAs are matter of great interest and debate at present.[5,6]

Nevertheless, the HEAs have generated considerable research attention due to their several attractive

*Corresponding author. Email: pinakib@iith.ac.in

and intriguing mechanical properties.[4,5,7–15] In order to further optimize the strength–ductility combination, multiphase HEAs consisting of ductile and hard phases have been suggested.[16] The development of non-equiatomic lamellar eutectic HEAs is a noteworthy approach in this direction.[16,17] It is envisaged that thermo-mechanical processing can further enhance the properties of these alloys,[18] but needs to be clarified in depth.

In the present work, the effect of heavy cold-rolling and annealing on microstructure and properties of EHEA is investigated for the first time. The target alloy with a nominal composition of $AlCoCrFeNi_{2.1}$ (elements in atomic ratios) was prepared by arc-melting a mixture of the constituent elements (purity better than 99.9%) in a Ti-gettered high-purity argon atmosphere. The melting was repeated at least five times to achieve a good chemical homogeneity of the alloy. The molten alloy was suction-cast into a 15 mm (width) × 90 mm (length) × 3 mm (thickness) copper mold. Small pieces (dimensions: 20 mm (length) × 15 mm (width)) were extracted from the as-cast material and subjected to multi-pass cold-rolling to ~90% reduction in thickness (final thickness ~300 μm) using a laboratory scale two-high rolling machine (Fenn, USA) having 140 mm diameter rolls. Samples for microstructural and tensile studies were obtained from the cold-rolled sheets and subsequently annealed at 800°C for 1 hour to obtain a fully recrystallized microstructure. The microstructural characterization of the samples at different length scales was carried out using electron backscatter diffraction (EBSD) system (Oxford Instruments, UK) mounted on a scanning electron microscope (Carl-Zeiss, Germany; Model: SUPRA 40) and transmission electron microscope (TEM) (JEOL 2010) operated at 200 KV. The samples for EBSD and TEM were prepared using standard electropolishing techniques (electrolyte: 90% ethanol + 10% perchloric acid). Tensile tests were carried out at ambient temperature using a floor-mounted testing machine (Shimadzu, Japan) using an initial strain rate of $8.3 \times 10^{-4}\ s^{-1}$.

The typical lamellar morphology of the as-cast alloy is seen in the large area EBSD phase map (Figure 1(a)) and in greater detail in the bright field TEM micrograph

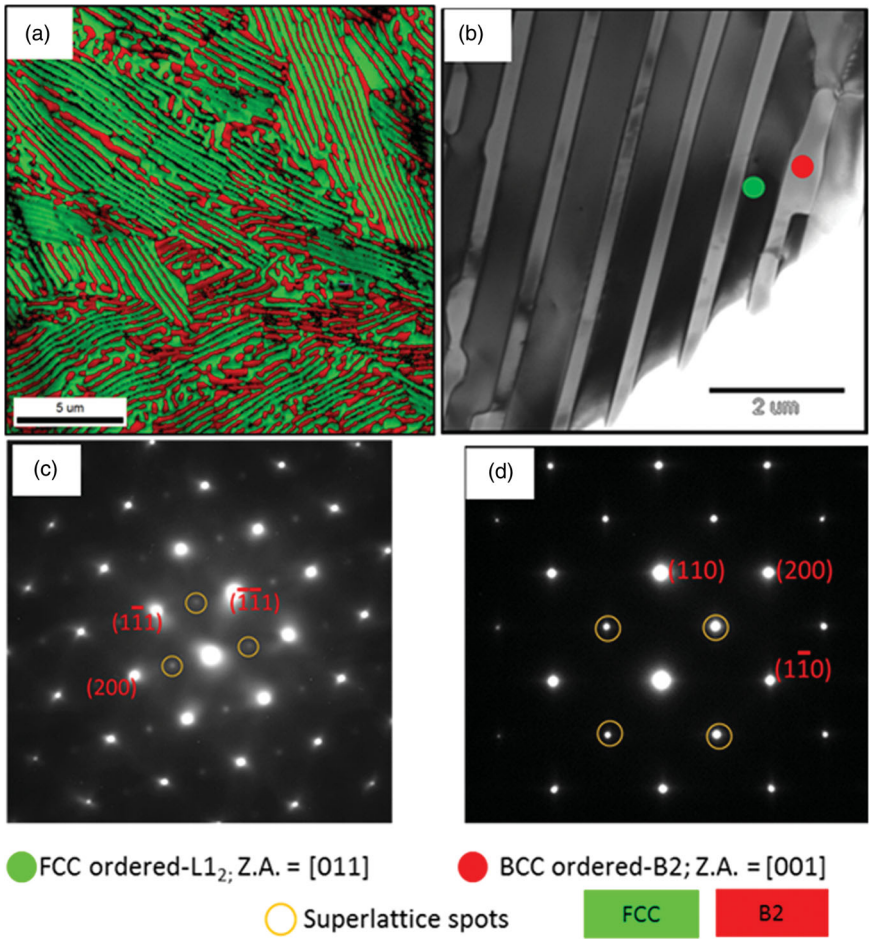

Figure 1. (Colour online) (a) EBSD phase map and (b) TEM micrograph of the as-cast alloy of $AlCoCrFeNi_{2.1}$ showing the lamellar structure; (c) and (d) are the SADPs obtained from the L12 phase the region marked by a green circle in (b) and B2 phase the region marked by a red circle in (b), respectively (Z.A. is abbreviated for zone axis).

(Figure 1(b)). The presence of weak superlattice spots (circled) in the TEM-SADPs (selected area diffraction patterns) (Figure 1(c)–(d)), obtained from the two phases (marked by green and red circles in Figure 1(b)), reveal ordered FCC ($L1_2$) (Figure 1(c)) and ordered BCC (B2) (Figure 1(d)) phases. The average thickness of the $L1_2$ and B2 lamellae (highlighted in green and red, respectively, in the phase map in Figure 1(a)) are ~0.57 and 0.20 μm, respectively, which agree quite well with those measured from TEM micrographs (Figure 1(b)). The volume fractions of the two phases are ~65% and 35%, respectively.

Figure 2(a) shows a typical EBSD band contrast map of the cold-rolled material. Presence of numerous shear bands can be easily identified (marked by arrows in Figure 2(a)), which leads to extensive fragmentation of the microstructure. Figure 2(b) shows the TEM micrograph of the 90% cold-rolled alloy obtained from the rolling plane (ND normal) section. The ring pattern of the SADP (Figure 2(c)) taken from the green circle position in (b) reveals the evolution of deformation induced ultrafine-grained (UFG) microstructure and transformation of the ordered $L1_2$ to disordered FCC during cold-rolling. The presence of weak superlattice spots in the SADP (Figure 2(d)) taken from the red circle position in (b) indicates that the B2 phase remains stable during cold-rolling. The periodical diffraction spots in Figure 2(d) also shows that the B2 phase is hard and is not heavily deformed.

The EBSD phase map (Figure 3(a)) and the TEM micrograph (Figure 3(b)) of the specimen 90% cold-rolled and annealed at 800°C reveal the development of an equiaxed duplex microstructure. The equiaxed grains of the two phases are fully recrystallized and dislocations are rarely observed in Figure 3(b). The SADPs of the two phases confirm the presence of equiaxed recrystallized grains having disordered FCC (Figure 3(c)) and ordered B2 (Figure 3(d)) structures. The average grain diameters of the FCC and B2 phases are quite similar (~0.60 μm), while the volume fractions of the two phases are ~55% and 45%, respectively. The phase map (Figure 3(a)) and TEM micrograph (Figure 3(b)) show the presence of profuse annealing twins inside the FCC grains.

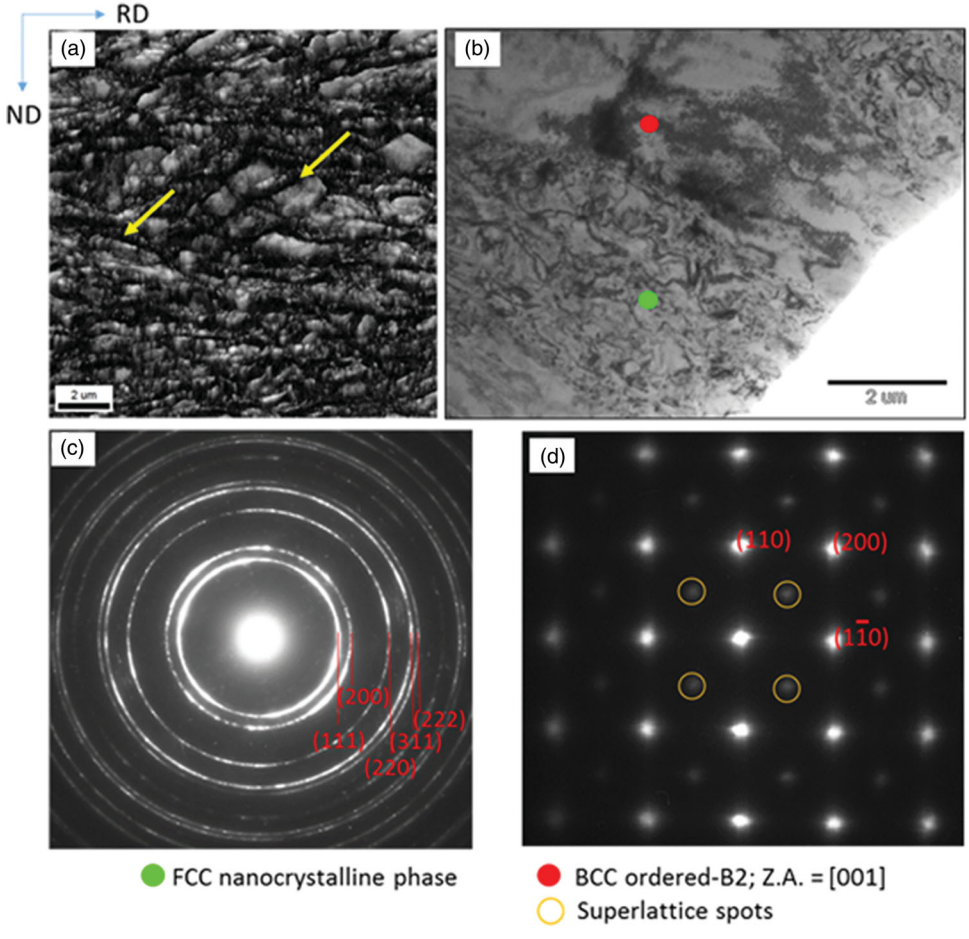

Figure 2. (Colour online) (a) EBSD band contrast map and (b) TEM micrograph (rolling plane) of the 90% cold-rolled material. The SADPs shown in (c) and (d) correspond to the ultrafine-disordered FCC phase (obtained from the region marked by a green circle in (b)) and B2 phase (obtained from the region marked by a red circle in (b)) phases, respectively.

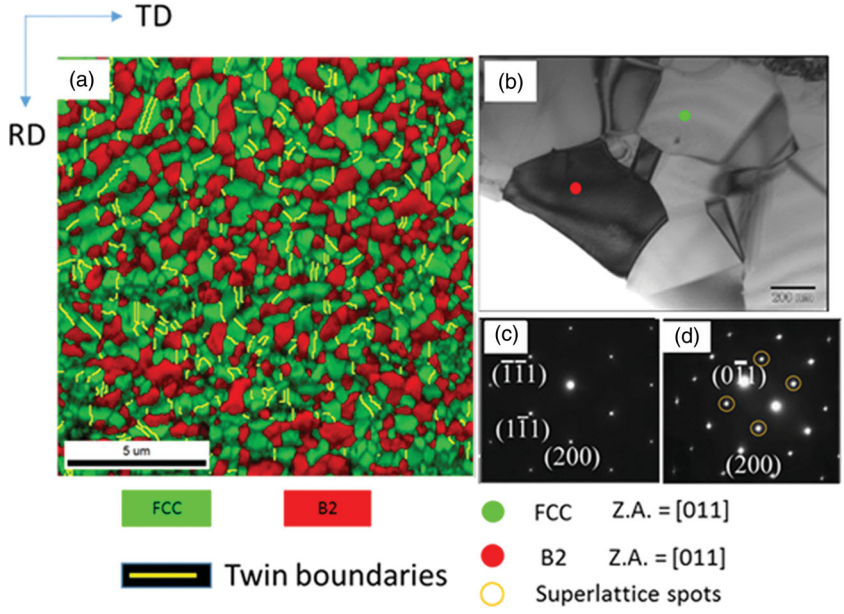

Figure 3. (Colour online) (a) EBSD phase map and (b) TEM micrograph (rolling plane) of the specimen 90% cold-rolled and annealed at 800°C. The SADPs shown in (c) and (d) correspond to ultrafine-disordered FCC (obtained from the region marked by a green circle in (b), corresponding to the green grains in (a)) and B2 (obtained from the region marked by a red circle in (b), corresponding to the red grains in (a)) phases, respectively.

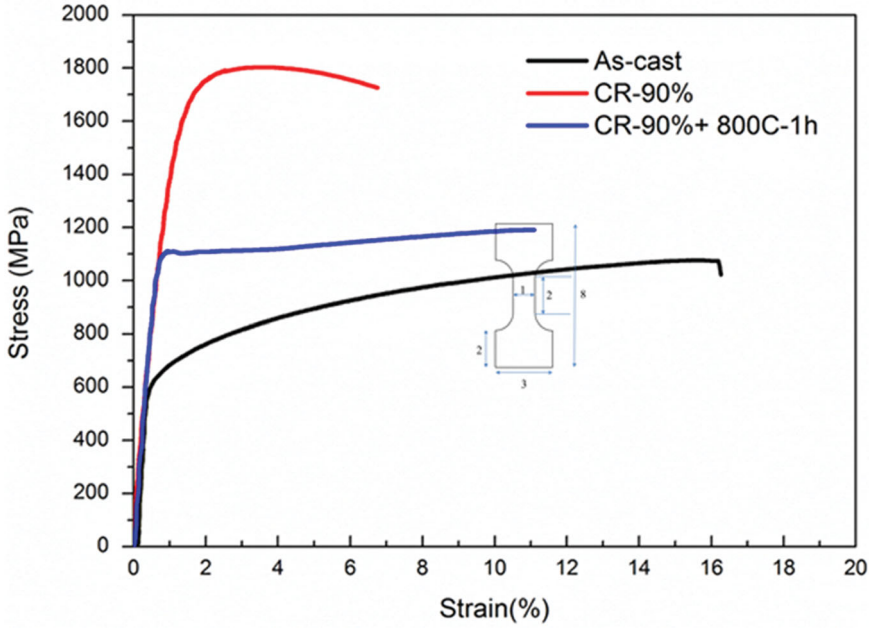

Figure 4. (Colour online) Engineering stress–strain curves of the $AlCoCrFeNi_{2.1}$ EHEA in the as-cast, cold-rolled and annealed conditions. The dimensions of the tensile specimen is shown inset (all dimensions in mm).

The tensile stress–strain curves of the specimens in the as-cast, cold-rolled and annealed conditions are shown in Figure 4. The as-cast alloy shows yield strength (YS) ~620 MPa and ultimate tensile strength (UTS) ~1050 MPa and elongation to failure (e_f) of 17%. Cold-rolling results in a drastic increase in YS to and UTS to ~1625 MPa and 1800 MPa, respectively, at the expense of elongation (e_f ~6%). The annealed material shows discontinuous yielding but a remarkable strength–ductility combination, having YS and UTS of 1100 and 1200 MPa, respectively and e_f ~12%.

The starting cast EHEA is having $L1_2$ as the major phase. Although the ordered phases generally have poor ductility, the $L1_2$ phase in the present EHEA could be heavily cold-rolled up to 90% reduction, leading to deformation induced ultrafine to nanostructure

formation. It has been well known that B-doped Ni_3Al with ordered $L1_2$ phase can be extensively cold-rolled at room temperature, accompanied by profuse shear band formation [19] and progressive disordering.[19,20] The successful heavy cold-rolling, high density of shear bands and disordering of the $L1_2$ phase (Figure 2(c)) of the present EHEA show evident similarities with the deformation behavior of B-doped Ni_3Al.

The development of UFG microstructures after annealing has been observed in single [21] and multiphase HEAs.[22,23] This has been attributed to their sluggish diffusion behavior that suppresses grain growth.[21] In addition to the sluggish diffusion effect, the finely fragmented microstructure of the present EHEA after cold-rolling should provide high density of potential nucleation sites for recrystallization in the subsequent annealing stage. Furthermore, the growth of one phase is inhibited by the presence of the other phase, typically observed in duplex alloys.[24] The change in the phase fraction observed after annealing is also found in other duplex alloys as the equilibrium phase fraction is determined by the annealing temperature.[25] The evolution of recrystallized UFG duplex microstructure in the EHEA thus appears to be quite consistent with these findings.

The high strength and ductility of the as-cast EHEA can be attributed to the fine lamellar microstructure. The large increase in strength after heavy cold-rolling at the expense of elongation is consistent with typical work-hardened metallic materials. It is noteworthy, however, that the cold-rolled specimen is not brittle but keeps a total elongation of $\sim$6%. Annealing of the cold-rolled specimen naturally decreases its strength, but the UFG duplex specimen shows a remarkable balance of strength and ductility. It should be noted that the yield and tensile strengths of the annealed specimen are higher than those of the as-cast specimen, even though the microstructural dimensions of the UFG duplex material are slightly coarser than those of the as-cast material. This is in contrast to FeNiMnAlCr alloy having lamellar microstructure, where strength after annealing is lower than the as-cast alloy due to structural coarsening.[23] The increase in strength after annealing as compared to the as-cast material is likely due to the increased fraction of the harder B2 phase [23] and equiaxed morphology of the UFG structure. The YS of this alloy in the annealed condition ($\sim$1100 MPa) is evidently much higher than other cold-rolled and annealed lamellar alloys such as FeNiMnAlCr ($\sim$600 MPa) [23] and $Al_{0.5}CrCuFeNi_2$ ($\sim$950 MPa).[18] The other interesting feature of the annealed UFG EHEA, that is, discontinuous yielding has been reported in various kinds of UFG materials,[26–29] although the mechanism is yet to be clarified fully.

The present results show that the UFG duplex microstructure can be successfully processed by heavy cold-rolling and annealing to tailor the mechanical properties of an $AlCoCrFeNi_{2.1}$ HEA showing a eutectic lamellar structure in the as-cast condition. It is envisaged that the present outcome should motivate the future studies on mechanical property improvement in other HEAs with ordered phases.

Disclosure Statement No potential conflict of interest was reported by the authors.

Funding This work has been supported by the DST, India [grant number SB/S3/ME-47/2013]; The Grant-in-Aid for Scientific Research (S) through Ministry of Education, Culture, Sports, Science and Technology (MEXT), Japan [grant number 15H05767]; and the startup grant from Areas of Advance Materials Science at Chalmers University of Technology and the Junior Researcher Grant from the Swedish Research Council [grant number 2015-04087]. The research leading to these results has received funding from the People Programme (Marie Curie Actions) of the European Union's Seventh Framework Programme (FP7/2007-2013) [REA grant agreement number 608743].

References

[1] Yeh JW, Chen SK, Lin SJ, et al. Nanostructured high-entropy alloys with multiple principal elements: novel alloy design concepts and outcomes. Adv Eng Mater. 2004;6:299–303.
[2] Yeh JW. Alloy design strategies and future trends in high-entropy alloys. JOM. 2013;65:1759–1771.
[3] Otto F, Yang Y, Bei H, George EP. Relative effects of enthalpy and entropy on the phase stability of equiatomic high-entropy alloys. Acta Mater. 2013;61:2628–2638.
[4] Yao MJ, Pradeep KG, Tasan CC, Raabe D. A novel, single phase, non-equiatomic FeMnNiCoCr high-entropy alloy with exceptional phase stability and tensile ductility. Scr Mater. 2014;72–73:5–8.
[5] Lu ZP, Wang H, Chen MW, et al. An assessment on the future development of high-entropy alloys: summary from a recent workshop. Intermetallics. 2015;66:67–76.
[6] Ye YF, Wang Q, Lu J, et al. High-entropy alloy: challenges and prospects. Mater Today. 2015 (in press).
[7] Zhang Y, Zuo TT, Tang Z, et al. Microstructures and properties of high-entropy alloys. Prog Mater Sci. 2014;61:1–93.
[8] Gludovatz B, Hohenwarter A, Catoor D, Chang EH, George EP, Ritchie RO. A fracture-resistant high-entropy alloy for cryogenic applications. Science. 2014;6201:1153–1158.
[9] Tsai MH, Yeh JW. High-entropy alloys: a critical review. Mater Res Lett. 2014;2:107–123.
[10] Miracle DB, Miller JD, Senkov ON, Woodward C, Uchic M, Tiley J. Exploration and development of high entropy alloys for structural applications. Entropy. 2014;16:494–525.
[11] Zhang Y, Zuo TT, Cheng YQ, Liaw PK. High-entropy alloys with high saturation magnetization, electrical resistivity and malleability. Sci Rep. 2013;3:1–7.
[12] Otto F, Dlouhy A, Somsen C, Bei H, Eggeler G, George EP. The influences of temperature and microstructure on the tensile properties of a CoCrFeMnNi high-entropy alloy. Acta Mater. 2013;61:5743–5755.

[13] Zhang Z, Mao MM, Wang J, et al. Nanoscale origins of the damage tolerance of the high-entropy alloy CrMnFeCoNi. Nat Commun. 2015;6:1–6.
[14] Zhang Y, Qiao JW, Liaw PK. A brief review of high entropy alloys and serration behavior and flow units. J Iron Steel Res Int. 2016;23(1):2–6.
[15] Gali A, George EP. Tensile properties of high- and medium-entropy alloys. Intermetallics. 2013;39:74–78.
[16] Lu Y, Dong Y, Guo S, et al. A promising new class of high-temperature alloys: eutectic high-entropy alloys. Sci Rep. 2014;4:1–5.
[17] He F, Wang Z, Cheng P, et al. Designing eutectic high entropy alloys of $CoCrFeNiNb_X$. J Alloys Compd. 2016;656:284–289.
[18] Ma SG, Qiao JW, Wang ZH, Yang HJ, Zhang Y. Microstructural features and tensile behaviors of the $Al_{0.5}CrCuFeNi_2$ high-entropy alloys by cold rolling and subsequent annealing. Mater Des. 2015;88:1057–1062.
[19] Ball J, Gottstein G. Large-strain deformation of $Ni_3Al + B$.1. Microstructure and texture evolution during rolling. Intermetallics. 1993;1:171–185.
[20] Jang JSC, Koch CC. Amorphization and disordering of the Ni_3Al ordered intermetallic by mechanical milling. J Mater Res. 1990;5:498–510.
[21] Bhattacharjee PP, Sathiaraj GD, Zaid M, et al. Microstructure and texture evolution during annealing of equiatomic CoCrFeMnNi high-entropy alloy. J Alloys Compd. 2014;587:544–552.
[22] Park N, Watanabe I, Terada D, Yokoyama Y, Liaw PK, Tsuji N. Recrystallization behavior of CoCrCuFeNi high-entropy alloy. Metall Mater Trans A. 2015;46:1481–1487.
[23] Baker I, Meng F, Wu M, Brandenberg A. Recrystallization of a novel two-phase FeNiMnAlCr high entropy alloy. J Alloys Compd. 2016;656:458–464.
[24] Ahmed MZ, Bhattacharjee PP. Evolution of microstructure and texture during isothermal annealing of a heavily warm-rolled duplex steel. ISIJ Int. 2014;54:2844–2853.
[25] Humphreys FJ, Hatherly M. Recrystallization and related annealing phenomena. 2nd ed. Oxford: Elsevier; 2004.
[26] Kamikawa N, Huang X, Tsuji N, Hansen N. Strengthening mechanisms in nanostructured high-purity aluminium deformed to high strain and annealed. Acta Mater. 2009;57:4198–4208.
[27] An XH, Wu SD, Zhang ZF, Figueiredo RB, Gao N, Langdon TG. Enhanced strength-ductility synergy in nanostructured Cu and Cu-Al alloys processed by high-pressure torsion and subsequent annealing. Scripta Mater. 2012;66:227–230.
[28] Li Z, Fu L, Fu B, Shan A. Yield point elongation in fine-grained titanium. Mater Lett. 2013;96:1–4.
[29] Saha R, Ueji R, Tsuji N. Fully recrystallized nanostructure fabricated without severe plastic deformation in high-Mn austenitic steel. Scripta Mater. 2013;68:813–816.